AGU PUBLICATIONS

Geophysical Research Letters

RESEARCH LETTER
10.1002/2014GL060781

Key Points:
- Voyager 1 is predicted to encounter the heliospheric current sheet again
- Such an encounter would demonstrate that Voyager 1 remains in the heliosheath

Correspondence to:
L. A. Fisk,
lafisk@umich.edu

Citation:
Gloeckler, G., and L. A. Fisk (2014), A test for whether or not Voyager 1 has crossed the heliopause, *Geophys. Res. Lett.*, *41*, 5325–5330, doi:10.1002/2014GL060781.

Received 5 JUN 2014
Accepted 3 JUL 2014
Accepted article online 18 JUL 2014
Published online 6 AUG 2014

A test for whether or not Voyager 1 has crossed the heliopause

G. Gloeckler[1] and L. A. Fisk[1]

[1]Department of Atmospheric, Oceanic, and Space Sciences, University of Michigan, Ann Arbor, Michigan, USA

Abstract The *Voyager* 1 spacecraft is currently in the vicinity of the heliopause, which separates the heliosphere from the local interstellar medium. There has been a precipitous decrease in particles accelerated in the heliosphere and a substantial increase in galactic cosmic rays (GCRs). The evidence is unclear, however, as to whether *Voyager* 1 has crossed the heliopause into the local interstellar medium or remains within the heliosheath. In this Letter we propose a test that will determine whether *Voyager 1* has crossed the heliopause: If *Voyager 1* remains in the heliosheath, the high densities observed must be due to compressed solar wind, with the consequence that *Voyager 1* will encounter another current sheet, where the polarity of the magnetic field reverses. *Voyager 1* observations can be used to predict that the next current sheet crossing is likely to occur during 2015.

1. Introduction

The *Voyager 1* spacecraft, hereafter referred to as *V1*, is currently in the vicinity of the heliopause, which separates the heliosphere from the local interstellar medium. There has been a precipitous decrease in particles accelerated in the heliosphere and a substantial increase in galactic cosmic rays (GCRs) [*Krimigis et al.*, 2013; *Stone et al.*, 2013], suggesting easy escape of the former across the heliopause and entry of the latter. The question is, has *V1* actually crossed the heliopause and is it now in the interstellar medium? Here the evidence is inconclusive. The direction of the magnetic field observed by *V1* is essentially unchanged from the direction of the heliosheath magnetic field [*Burlaga et al.*, 2013] and is in a substantially different direction from the expected direction of the interstellar magnetic field inferred from *IBEX* observations of energetic neutral atoms (ENAs) [*McComas et al.*, 2009, 2012, and references therein], from SOHO observations of the deflection of the neutral hydrogen flow relative to that of helium [*Lallement et al.*, 2005], as well as from observations of the polarization of interstellar grains [*Frisch*, 2011]. However, *Gurnett et al.* [2013] observe plasma oscillations at 122.2, 122.5, and 123.9 AU, which are a direct measure of the plasma electron density, and find densities of 0.055, 0.058, and 0.083 cm^{-3}, respectively. These densities are comparable to densities expected in the local interstellar medium and are much larger than the plasma densities observed by the working plasma detector on *Voyager 2* (hereafter referred to as *V2*) closer to the termination shock [*Richardson*, 2008].

In this Letter we propose a simple test that will determine whether *V1* remains in the heliosheath or has already crossed the heliopause into the local interstellar medium. The test is based on two principles:

1. One of the most observable features of the heliosphere, which would clearly identify that *V1* remains in the heliosheath, is a current sheet crossing. The heliosphere contains a single large current sheet, which separates two hemispheres of opposite magnetic polarity. As the solar cycle evolves, the current sheet becomes highly tilted relative to the solar equatorial plane and appears to rotate through the poles of the Sun, accomplishing the polarity reversal of the dipole component of the solar magnetic field. Warps in the current sheet will be compressed as the current sheet is convected into the distant heliosheath, where the radial solar wind speed becomes very small. Magnetic reconnection will then occur, resulting in two regions of opposite polarity, with reduced magnetic strength due to the reconnection. The single current sheet that separates these two regions marks the time where the field reversal of the Sun occurred at that heliographic latitude and radius.
2. If *V1* remains in the heliosheath, the large densities observed by *Gurnett et al.* [2013] must be the result of compressed solar wind. If the solar wind is compressed, it must be the result of a reduced flow velocity of the solar wind, particularly a reduced radial flow velocity. *V1* is thus moving faster than the outward flow of the solar wind and will encounter additional current sheets, where the polarity of the magnetic field reverses.

Here we calculate the likely distance at which *V1* will encounter the next current sheet. This distance can be estimated from *V1* observations and thus provides a clear test for whether *V1* remains in the heliosheath.

Fisk and Gloeckler [2014] have developed a detailed model for the nose region of the heliosheath, the region of the heliosheath in the direction of motion of the Sun through the local interstellar medium, the regions that the *Voyagers* are exploring. The model is based on two principles: (1) in the heliosheath, the dominant pressure results from the pickup ions and ACRs; and (2) beyond ~110 AU, the flow of the solar wind inferred from >40 keV anisotropy observations (the technique used to determine the solar wind velocity in the absence of a working plasma detector on *V1*) [*Krimigis et al.*, 2011; *Decker et al.*, 2012] is primarily in the radial and azimuthal directions, not in the polar direction. The model predicts that the solar wind is compressed and also yields the likely distance to the heliopause, as well as the likely properties of the heliopause. For our purposes here, the details of the model of *Fisk and Gloeckler* [2014] are not needed, other than to note that it is possible to construct a complete model for the nose region of the heliosheath in which the solar wind is compressed.

We begin by presenting the arguments for why it is both possible and indeed to be expected that the solar wind is compressed at the current location of *V1*. We then use *Voyager* observations to predict when *V1* is likely to encounter another current sheet. In Concluding Remarks we draw on the work of *Fisk and Gloeckler* [2014] and discuss the different behavior of energetic particles that should be expected when *V1* enters a region of opposite magnetic polarity.

2. The Argument for Compressed Solar Wind

The nose region of the heliosheath is a subsonic region, and thus the particle pressure is expected to be constant. It is sometimes argued that since particle density and pressure are related to each other through an equation of state, the solar wind density should also be constant in the nose region of the heliosheath, i.e., it cannot be compressed. However, the nose region of the heliosheath is not a conventional plasma.

The particle pressure in the nose region of the heliosheath is the result of the mobile interstellar pickup ions and particles accelerated in the heliosheath (usually referred to as anomalous cosmic rays (ACRs)) and is readily modeled and/or observed: (1) The pickup process in the supersonic solar wind is readily modeled and yields the pressure in pickup ions upstream of the termination shock. Observations by the working plasma detector on *V2* find that it is primarily the pickup ions that are heated at the termination shock, satisfying the Rankine-Hugoniot relationship, which determines the pickup ion pressure in the heliosheath [*Richardson*, 2008]. This pickup ion pressure is validated by the *IBEX* observations of energetic neutral atoms resulting from the pickup ions [*Gloeckler and Fisk*, 2010]. (2) As for the energetic particles observed in the nose region of the heliosheath, at ~117 AU the differential intensity spectrum of, e.g., ACR oxygen has a spectral index of −1.5, with an exponential rollover, as is expected from the pump acceleration mechanism of *Fisk and Gloeckler* [2013]. For such a spectrum, the pressure is due primarily to particles with energies that are measured by the Cosmic Ray Subsystem (CRS) detector on *V1* [*Stone et al.*, 2013], and thus the ACR pressure is readily determined. The combined pressure in the pickup ions (deduced from *IBEX* observations) and in the ACRs (measured by *V1* at distances of ~118 AU) is $\sim 1.2 \times 10^{-12}$ dyne cm^{-2} [*Gloeckler and Fisk*, 2010].

The pressure in the pickup ions and ACRs is the dominant pressure in the nose region of the heliosheath. The plasma detector on *V2*, which is closer to the termination shock than *V1*, measures both the ram pressure and the thermal pressure of the solar wind [*Richardson*, 2008]. While the temperature of the solar wind increases by about a factor of 10 crossing the termination shock [*Richardson*, 2008], the pressure in the pickup ions and ACRs is a factor of ~3 larger than the ram pressure, and a factor of ~15 larger than the thermal pressure of the solar wind. Relative to itself, the solar wind remains supersonic in the heliosheath.

The hot pickup ions, and particularly the energetic ACRs, have average speeds very much larger than the thermal speeds of the solar wind. As is discussed in detail in *Fisk and Gloeckler* [2014], the pickup ions and ACRs should flow freely along the magnetic field and seek to maintain pressure equilibrium in the nose region of the heliosheath, independent of the local conditions in the solar wind. Thus, in the nose region of the heliosheath we have two distinct and basically uncoupled gases: the mobile pickup ions and ACRs, which contain the pressure, and the relatively cold thermal solar wind, which contains the mass. The pickup ions and ACRs are responding to the global conditions in the heliosheath as they attempt to maintain pressure

equilibrium. The solar wind is flowing into the heliosheath across the termination shock, and its density is responding to local conditions. The solar wind by itself has an equation of state that relates pressure and density, and the same is true for the pickup ions and ACRs. However, it is inappropriate to consider the combined gas of pickup ions, ACRs, and solar wind as having an equation of state since the pressure is determined by global conditions and the density by local conditions. There is thus no restriction on compressing the solar wind.

We should in fact expect that the solar wind must be compressed at distances at least out to ~122 AU, simply from the solar wind velocity measurements. Although *V1* does not have a functional plasma detector, *Krimigis et al.* [2011] and *Decker et al.* [2012] have been able to infer the solar wind flow velocity from the convective anisotropy of >40 keV ions and find with their low-energy charged particle (LECP) detector that the inferred radial flow speed decreases systematically to a very small value beyond ~113 AU, with a small azimuthal speed persisting. At distances between ~116 and ~120 AU from the Sun, *V1* was rotated at a number of short time intervals to observe the anisotropies of low-energy ions in a direction normal to the usual azimuthal rotation of LECP [*Decker et al.*, 2012]. At these distances the anisotropies, and thus the inferred convective flow speed in the polar direction, were found to be small, with an average of essentially zero [*Decker et al.*, 2012]. This result is consistent with that of *Stone and Cummings* [2011], who observe, using the Cosmic Ray Subsystem (CRS) detector that measures somewhat higher energy particles, that the anisotropies in the polar direction become increasingly small with distance into the heliosheath.

The *V1* solar wind observations can only be made when there are low-energy energetic particles present, from which the convective anisotropies can be determined. The measurements cease at ~122 AU, when the particles accelerated in the heliosheath escape. However, inside this distance, where the solar wind flow velocity becomes small in all directions, the continuity of mass equation requires that the solar wind is compressed, and its density increases substantially. Beyond 122 AU there are no solar wind measurements on *V1*, but it is reasonable to assume that however small, the solar wind continues to flow radially outward, since otherwise the solar wind density would increase without bound.

3. Prediction of When *V1* Will Encounter Another Current Sheet

In this section we present our prediction as to when *V1* will encounter another current sheet crossing. Our prediction is based primarily on the radial dependence of the average radial component of the solar wind speed, $<u_r(r)>$, for which no direct measurements exist on *V1*. We determine $<u_r(r)>$ from several indirect measurements, which taken together constrain when *V1* should encounter the next current sheet.

3.1. The Average Radial Speed of the Solar Wind From 1 to ~113 AU

Starting in the inner heliosphere, $<u_r(r)>$ gradually decreases [*Richardson et al.*, 2008; *Gloeckler et al.*, 1997; *Lee*, 1997] due to the process of picking up recently ionized interstellar neutral gas, to a smaller value immediately upstream of the termination shock at r_{ts}, the distance at which the solar wind ram pressure (determined by the upstream speed) roughly balances the component of the pressure of the Local Interstellar Cloud (LIC) normal to the heliopause [e.g., *Gloeckler et al.*, 1997]. The normal component of the LIC pressure will vary with latitude and longitude.

Upon crossing the termination shock at r_{ts}, $<u_r(r)>$ decreases by the termination shock compression ratio, which is measured to be ~3 by both *V1* and *V2*. The compression ratio will likely be somewhat lower at solar maximum (a lower upstream speed) and somewhat higher at solar minimum (a higher upstream speed).

Further downstream of r_{ts}, out to ~117 AU, $<u_r(r)>$ can be reliably estimated from the LECP observations of *Krimigis et al.* [2011] and *Decker et al.* [2012]. The radial component of the solar wind speed is inferred from anisotropy measurements of >40 keV ions and, as shown in Figure 1, shows quasi-periodic variations, $\delta u_r(t,r)$, with time of about ±20 km/s over distance scales of several AU around a decreasing value of $<u_r(r)>$. Thus, *V1* measures $<u_r(r)> \pm \delta u_r(t,r)$.

Note that $<u_r(r)>$ decreases approximately linearly in Figure 1 to where the variations, $\delta u_r(t,r)$, are larger than $<u_r(r)>$ and can even result in negative radial solar wind flows. In this region, beyond ~113 AU, where the variations exceed the mean, we cannot use LECP observations directly and require another technique to infer $<u_r(r)>$. For $<u_r(r)>$ between 105 and 112.5 AU we can reliably use a linear fit to the LECP data.

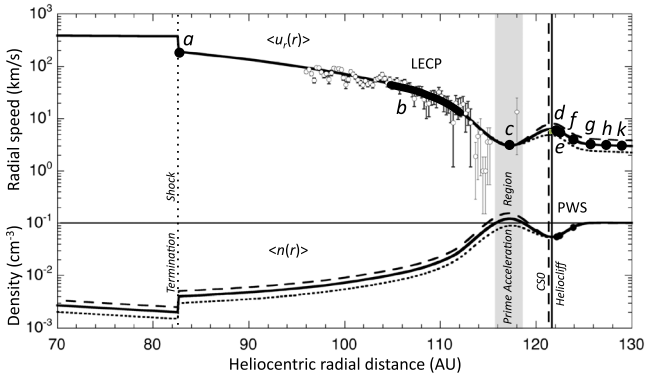

Figure 1. Variation of the average radial speed component, $<u_r(r)>$, and the associated average number density, $<n(r)>$, of the solar wind with heliocentric distance r. The termination shock is at heliocentric distance r_{ts}, which depends on and will vary with the solar wind speed upstream of the shock. Equation (2), with n_{ts}, the density just downstream to the termination shock, relates $<n(r)>$ to $<u_r(r)>$. A smooth variation of $<u_r(r)>$ with r (no abrupt changes) is achieved using a cubic spline fit through point a just downstream of the TS, line segment b (the linear fit to the low-energy charged particle (LECP) data from 105 to 112.5 AU), point c at ~117 AU (in the prime acceleration region) and points d, f, and g (speeds derived from PWS densities) and points h and k (speeds derived from Local Interstellar Medium densities). The speed at c is adjusted until the CS0 trajectory (see Figure 2b) goes through point X^*. The dashed, solid, and dotted curves correspond to values of n_{ts} of 0.005, 0.004, and 0.003 cm^{-3}, respectively. It is worth remarking that the solar wind is already highly compressed in the heliosheath, reaching a very high density at ~117 AU. At the heliocliff the density reached a local minimum, about a factor of two below the Local Interstellar Medium density.

3.2. The Average Radial Speed of the Solar Wind From ~113 to 121.31 AU

As the current sheet responsible for the reversal in the magnetic field polarity is convected outward with the solar wind, it will encounter *V1* twice. First, in the supersonic solar wind, where the current sheet is moving faster than *V1*, the current sheet overtakes *V1* at time t and distance r. Then, since $<u_r(r)>$ decreases with r (see Figure 1) to values below the speed of *V1* (~17 km/s), *V1* will overtake the same current sheet at time t^* and distance r^*. Fitting the related current sheet crossings observed by *V1* places strong constraints on the radial dependence of $<u_r(r)>$ and can be used to determine $<u_r(r)>$ in the region beyond 113 AU.

We use the last current sheet crossing observed by *V1*, labeled CS0 by *Burlaga et al.* [2013], which occurred at $t^*_{CS0} = 2012.57$ and $r^*_{CS0} = 121.31$ AU to determine the lower limit on the mean average radial speed between ~113 and 121.31 AU, which should give an estimate of the latest arrival times of the next polarity reversal. This is the current sheet crossing that occurred just before the "heliocliff," where there was a precipitous decrease in the ACRs. As can be seen in Figure 2a (dashed curve crossing zero), the first crossing of CS0, when it overtook *V1*, occurred sometime during DOY 135 in 2000 (14 May 2000, $t_{CS0} = 2000.3662$) with *V1* at 77.48 AU; a close examination of the daily averages of the magnetic field direction showed an abrupt change in direction at hour 19 of 14 May 2000 (http://vgrmag.gsfc.nasa.gov/data.html).

By recalling that beyond ~110 AU the flow of the solar wind is primarily in the radial and azimuthal directions, the trajectory (distance versus time) of CS0 is calculated using the following simple equation:

$$t(r) = t_0 + \int_{r_0}^{r} \frac{dr}{\langle u_r(r) \rangle}. \quad (1)$$

We assume that the solar wind speed at 1 AU is 455 km/s, an appropriate solar maximum value, consistent with the 453 km/s speed measured by *Ulysses* at the *V1* latitude at approximately the same time (2 December 1999) (http://omniweb.gsfc.nasa.gov/coho/). We assume that out to 112.5 AU $<u_r(r)>$ is determined as described in section 3.1. Then, by requiring that the trajectory must pass through both (t_{CS0}, r_{CS0}) and (t^*_{CS0}, r^*_{CS0}), we find a mean radial speed of $<u_r(r)> = 4.3$ km/s in the region from ~113 to 121.31 AU. Note that this calculation is particularly sensitive to the value of $<u_r(r)>$ between 113 and 121 AU since with this slow speed, the dwell time of the current sheet in this region is long.

It is unlikely that $<u_r(r)>$ is constant at 4.3 km/s from ~113 to 121.31 AU, since this would result in an abrupt change in $<u_r(r)>$ at ~113 AU. In subsequent calculations we will make the transition of $<u_r(r)>$ smooth across ~113 AU (see caption to Figure 1). The trajectory of CS0 is shown in Figure 2b. As required, it goes through points X (t_{CS0}, r_{CS0}) and X^* (t^*_{CS0}, r^*_{CS0}).

3.3. The Average Radial Speed of the Solar Wind Beyond 121.31 AU

Using observations of plasma oscillations, *Gurnett et al.* [2013] report very accurate measurements of the plasma electron density during three short time intervals when *V1* was at 122.155, 122.465, and 123.910 AU,

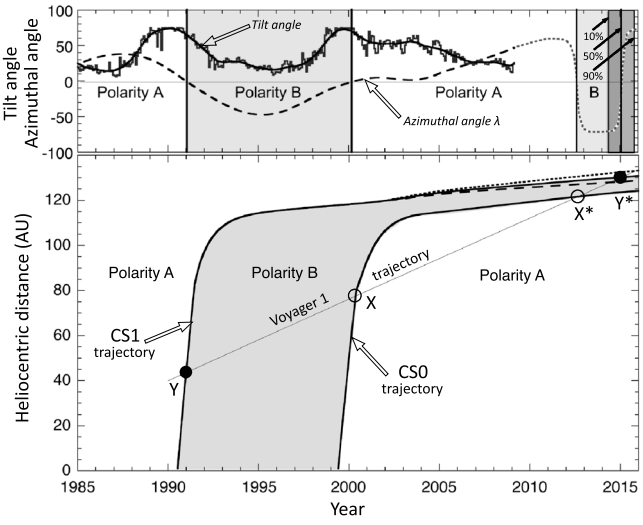

Figure 2. (top) Variations with time of the maximum extent of the tilt angle in the northern hemisphere [*Hoeksema*, 1995, http://wso.stanford.edu/Tilts.html] during a Carrington rotation (step curve) and the 28% weighted average of the azimuthal angle, λ, (in the RTN coordinate system) of the magnetic field (dashed curve) observed by Magnetometer on *Voyager 1*. The solid curve is the 5% weighted average of the step curve. The dotted curve is an extrapolation of the average azimuthal magnetic angle beyond 2009. The dominant polarity reverses when λ (dashed or dotted curve) crosses zero. This reversal should coincide with the rotation of the current sheet past 90° observed at 1 AU about a year earlier. However, finding the exact time when the rotation through 90° at 1 AU occurred is difficult because estimates of large tilt angles have large uncertainties. The times of the next current sheet crossing by *V1* are indicated by the vertical lines labeled 10% (probability), 50%, and 90%. (bottom) Trajectories of current sheet crossings CS0 (observed) and CS1 (predicted). Even though numerous current sheet crossings were observed by *V1* from 1991 to 2012.57 (between points *Y* and *X**), none were seen after the CS0 crossing at *X**. The most plausible explanation is that magnetic reconnection occurs beyond ~122 AU, where the solar wind speed is very small, as discussed in the text.

respectively. The measured densities are shown in Figure 1. The corresponding radial solar wind speed, assuming that the density, *n*, measured by *Gurnett et al.* [2013] is due to compressed solar wind, can be found from the continuity of mass equation,

$$\langle u_r(r)\rangle = \frac{n_{ts} r_{ts}^2 u_{ts}}{n(r) r^2}. \qquad (2)$$

In the model of *Fisk and Gloeckler* [2014], the density of the solar wind at radial distances beyond where *Gurnett et al.* [2013] observed is assumed to have a value equal to the interstellar density. The solar wind density is maintained at this value due to the nature of the heliopause and the pressure in the LIC. We take the solar wind density beyond ~124 AU to be constant at ~0.1 cm^{-3}, in which case, in this region, $<u_r(r)>$ decreases as r^{-2}.

3.4. The Profile of the Average Radial Speed of the Solar Wind

Taking the results of sections 3.1–3.3 together, and providing smooth transitions across the boundaries between the regions considered, yields the profile of the average radial speed of the solar wind shown in Figure 1, out to 130 AU. The parameters used in determining this profile can be varied, only within fairly narrow limits, as we consider below. Also shown in Figure 1 is the density profile calculated from equation (2). Note that there is a region just inside the heliocliff where the density reaches a maximum. It is interesting to note that the density maximum occurs at the location of prime acceleration of ACRs, where they reach their maximum energies [*Stone et al.*, 2013].

3.5. The Prediction of When *V1* Will Encounter the Next Current Sheet

As discussed in section 3.2, current sheet CS0, which *V1* observed at $t^*_{CS0} = 2012.57$ and $r^*_{CS0} = 121.31$ AU, was the same current sheet that overtook *V1* at $t_{CS0} = 2000.367$ and $r_{CS0} = 77.48$ AU. It follows then that the next current sheet that *V1* should encounter is the current sheet that overtook *V1* during the previous change in the polarity of the solar magnetic field, which, as can be seen in Figure 2a, occurred at $t_{CS1} = 1990.996$ when *V1* was at $r_{CS1} = 43.54$ AU.

Using the date and location of this initial encounter of *V1* with CS1, and the average radial speed of the solar wind in Figure 1 (to which we can make small adjustments in the parameters, particularly in the density at the termination shock, n_{ts}), we can estimate when *V1* will next encounter CS1. A lower limit on when the encounter will occur is obtained by noting that *V1* has not yet overtaken CS1 (see quick look data at http://vgrmag.gsfc.nasa.gov/data.html), and thus $t^*_{CS1} >$ ~2014.4, which implies that $<u_r(r)>$ at 122.155 AU is greater than ~4.65 km/s. This speed condition is satisfied with a solar wind density just downstream of the termination shock of $n_{ts} = 0.003$ cm^{-3}, which is reasonable for solar maximum conditions. To estimate the upper limit on $<u_r(r)>$ we take the solar wind density just downstream of the termination shock to be

0.005 cm^{-3} which yields $<u_r(r)>$ at 122.155 AU of 7.85 km/s. Finally, a density just downstream of the termination shock of 0.004 cm^{-3} (a reasonable value for solar maximum conditions) yields $<u_r(r)>$ at 122.155 AU of 6.13 km/s.

Shown in Figure 2 are three trajectories of CS1 with values for n_{ts} of 0.003, 0.004, and 0.005 cm^{-3}, the dashed, solid, and dotted curves, respectively. The times when the trajectories of *V1* and CS1 cross are 2014.43, 2015.07, and 2015.87, respectively.

Based on our analysis, the probability of *V1* overtaking CS1 on 6 June 2014, 26 January 2015, and 14 November 2015 is 10%, 50%, and 90%, respectively.

4. Concluding Remarks

In this Letter we have provided a test of whether *V1* has crossed the heliopause or still remains in the heliosheath. If *V1* remains in the heliosheath, the high density measurements of *Gurnett et al.* [2013] must be due to compressed solar wind, which should result from a very slow outward radial flow speed, from which it is possible to predict that *V1* will most likely encounter another current sheet crossing during 2015.

The approach taken in this paper, that it is possible to compress the solar wind, is based upon the detailed model of *Fisk and Gloeckler* [2014]. In this model there is also a prediction that ACRs and GCRs will behave differently when the magnetic field polarity reverses. The model predicts that when the heliosheath magnetic field is oriented in the same general direction as the interstellar magnetic field, the two fields can merge beyond the heliopause, yielding easy escape of ACRs and easy entry of GCRs. This is apparently the case with the magnetic polarity that *V1* is now observing. When the heliosheath magnetic field is oriented generally opposite to the interstellar magnetic field, reconnection should occur beyond the heliopause, reconnection islands will form, and escape of the ACRs, and certainly entry of GCRs will be restricted.

Thus, if *V1* encounters another current sheet, it will provide strong observational evidence that the heliopause has not yet been crossed. If the region beyond the current sheet, with opposite magnetic polarity, is accompanied by less escape of ACRs and restricted entry of GCRs, it will be strong observational evidence for the model of *Fisk and Gloeckler* [2014].

Acknowledgments
This work was supported in part by NASA Grant NNX10AF23G and by NSF Grant AGS-1043012. In compliance with AGU Data Policy, all data used in this paper are available from the references cited.

The Editor thanks two anonymous reviewers for assistance in evaluating this manuscript.

References

Burlaga, L. F., N. F. Ness, and E. C. Stone (2013), Magnetic field observations of Voyager 1 entered the heliosheath depletion region, *Science*, *341*, 147–150.

Decker, R. B., S. M. Krimigis, E. C. Roelof, and M. E. Hill (2012), No meridional plasma flow in the heliosheath transition region, *Nature*, *489*, 124–127.

Fisk, L. A., and G. Gloeckler (2013), The global configuration of the heliosheath inferred from recent Voyager 1 observations, *Astrophys. J.*, *776*, 79.

Fisk, L. A., and G. Gloeckler (2014), On whether or not Voyager 1 has crossed the heliopause, *Astrophys. J.*, *789*, 41.

Frisch, P. C. (2011), How local is the local interstellar magnetic field, in *Physics of the Heliosphere: A 10 Year Retrospective, AIP Conf. Proc.*, vol. 1436, edited by J. Heerikhuisen et al., 295 pp., AIP, N. Y.

Gloeckler, G., and L. A. Fisk (2010), Proton velocity distributions in the inner heliosheath derived from energetic hydrogen atoms measured with Cassini and IBEX, in *Pickup Ions Throughout the Heliosphere and Beyond, AIP Conf. Proc.*, vol. 1302, edited by J. A. le Roux et al., 110 pp., AIP, Melville, N. Y.

Gloeckler, G., L. A. Fisk, and J. Geiss (1997), Anomalously small magnetic field in the local interstellar cloud, *Nature*, *386*, 374–377.

Gurnett, D. A., W. S. Kurth, L. F. Burlaga, and N. F. Ness (2013), In situ observations of interstellar plasma with Voyager 1, *Science*, *341*, 1489–1492.

Hoeksema, J. T. (1995), The large-scale structure of the heliosheath current sheet during the Ulysses epoch, *Space Sci. Rev.*, *72*, 137–148.

Krimigis, S. M., E. C. Roelof, R. B. Decker, and M. E. Hill (2011), Zero outward flow velocity for plasma in a heliosheath transition layer, *Nature*, *474*, 359–361.

Krimigis, S. M., R. M. Decker, E. C. Roelof, M. E. Hill, T. P. Armstrong, G. Gloeckler, D. C. Hamilton, and L. J. Lanzerotti (2013), Search for the exit: Voyager 1 at Heliosphere's border with the galaxy, *Science*, *341*, 144–147.

Lallement, R., E. Quemerais, J. L. Bertaux, S. Ferron, D. Koutroumpa, and R. Pellinen (2005), Deflection of the interstellar neutral hydrogen flow across the heliospheric interface, *Science*, *307*, 1447–1449.

Lee, M. A. (1997), Effects of cosmic rays and interstellar gas on the dynamics of a wind, in *Cosmic Winds and the Heliosphere*, edited by J. R. Jokippi et al., pp. 857, Univ. of Arizona Press, Tucson, Ariz.

McComas, D. J., et al. (2009), Global observations of the interstellar interaction from the Interstellar Boundary Explorer (IBEX), *Science*, *326*, 959–962.

McComas, D. J., et al. (2012), The first three years of IBEX observations and our evolving heliosphere, *Astrophys. J. Suppl.*, *203*, doi:10.1088/0067-0049/203/1/1.

Richardson, J. D. (2008), Plasma temperature distributions in the heliosheath, *Geophys. Res. Lett.*, *35*, L23104, doi:10.1029/2008GL036168.

Richardson, J. D., Y. Liu, C. Wang, and D. J. McComas (2008), Determining the LIC H density from the solar wind slowdown, *Astron. Astrophys.*, *491*(1), 1–5.

Stone, E. C., and A. C. Cummings (2011), Voyager observations in the heliosheath: A quasi-stagnation region beyond 113 AU, in *Proceedings of the 32nd International Cosmic Ray Conference*, vol. 12, 29 pp., IUPAP, Beijing, China.

Stone, E. C., A. C. Cummings, F. B. McDonald, B. C. Heikkila, N. Lal, and W. R. Webber (2013), Voyager 1 observes low-energy galactic cosmic rays in a region depleted of interstellar ions, *Science*, *341*, 150–153.